Arabian Journal of Chemistry (2021) **14**, 103212

King Saud University

Arabian Journal of Chemistry

www.ksu.edu.sa
www.sciencedirect.com

ORIGINAL ARTICLE

Exploring the anticancer effects of tin oxide nanoparticles synthesized by pulsed laser ablation technique against breast cancer cell line through downregulation of PI3K/AKT/mTOR signaling pathway

Yingchang Guo [a,*], Yongli Zhao [a], Xiaobo Zhao [a], Shanshan Song [b], Bai Qian [c,*]

[a] *Department of Interventional Radiology, the First Affiliated Hospital, Xinxiang Medical University, Xinxiang 453100, Henan, China*
[b] *Department of Endocrinology, the First Affiliated Hospital, Xinxiang Medical University, Xinxiang 453100, Henan, China*
[c] *Department of Anesthesiology, The Second Affiliated Hospital of Zhengzhou University, Zhengzhou, China*

Received 17 March 2021; accepted 8 May 2021
Available online 15 May 2021

KEYWORDS

Tin oxide;
Nanoparticle;
Pulsed laser ablation technique;
Breast cancer cells;
Signaling pathway

Abstract Tin oxide nanoparticles (SnO_2 NPs) demonstrate potential anti-cancer functions. However, the anti-cancer mechanisms of SnO_2 NPs have not been explored in detail. In the present study, we synthesized SnO_2 NPs through laser ablation technique and examined their anticancer mechanisms and the probable involvement of the PI3K/AKT mediated pathways in human breast cancer cells (MCF-7) in vitro. The synthesized SnO_2 NPs were characterized by transmission electron microcopy (TEM), dynamic light scattering (DLS), and Fourier-transform infrared spectroscopy (FTIR) techniques. Afterwards, the breast cancer cells were incubated with increasing concentrations of SnO_2 NPs, and inhibition of cell proliferation was assessed by the viability assay. Furthermore, the quantification of reactive oxygen species (ROS) and apoptosis were examined by flow cytometry followed by superoxide dismutase (SOD) and catalase (CAT) activity as well as mitochondrial membrane potential assays. The expression levels of phosphoinositide 3-kinase (PI3K), protein kinase B (AKT), mechanistic target of rapamycin (mTOR), B-cell lymphoma 2 (Bcl-2), and Bax were also assessed by western blot and quantitative real time PCR (qRT-PCR). It was shown that SnO_2 NPs, 30 nm, with potential colloidal stability selectively prevented the proliferation of MCF-7 in comparison with MCF-10A cells and triggered ROS production, apoptosis,

* Corresponding authors at: NO.88, Health Road, Weihui, Xinxiang 453100, China (Y. Guo).
E-mail addresses: guoyingchang12@126.com (Y. Guo), baiqian@zzu.edu.cn (B. Qian).
Peer review under responsibility of King Saud University.

Production and hosting by Elsevier

https://doi.org/10.1016/j.arabjc.2021.103212

deactivation of SOD and CAT activity, and mitigation of mitochondrial membrane potential. Moreover, SnO_2 NPs stimulated mitochondrial-mediated apoptosis pathway by overexpression of Bax/Bcl-2 and downregulation of p-PI3K/p-AKT/p-mTOR signaling pathway. This data elucidates the possible mechanisms by which SnO_2 NPs may stimulate their anticancer effects.

1. Introduction

Despite the use of treatment strategies such as surgery, chemotherapy and radiotherapy, the mortality rate in patients with breast cancer is still high, which indicates the ineffectiveness of these treatment strategies (Abdel-Rahman, 2018). The destructive effect of chemotherapy and radiation therapy on normal cells is also one of the other disadvantages of this type of treatment (Brundha et al., 2019). Development of nano-based platforms that have anticancer properties is effective in preventing and reducing the incidence of cancer (Ansari et al., 2020; Khan et al., 2020; Khan et al., 2020). According to the mentioned points, in recent years, the tendency to use nanoparticles (NPs) with anticancer properties is increasing (Ansari et al., 2020; Khan et al., 2020; Khan et al., 2020). Among these, tin oxide (SnO_2) NPs have been identified as one of the most effective anticancer compounds due to their appropriate efficacy and potential compatibility at low concentrations (Ahmadabad et al., 2021). For example, it has been shown that SnO_2 NPs show potential albumin binding and anticancer effects activity against MCF-7 cells (Ahmadabad et al., 2021). Also, it has been shown that SnO_2 NPs can be developed as promising anticancer platforms against cervical carcinoma (Ma et al., 2020).

There are different methods of nanomaterial synthesis such as physical or chemical vapor deposition, sol-gel, pulsed laser ablation, thermolysis, and solution combustion (Kolahalam et al., 2019).

In the last few decades, the fabrication of a wide range of NPs by pulsed laser ablation method in liquid phase has received a great deal of interest in different biomedical areas (Honda et al., 2017; Musaev et al., 2013). Actually, relative to other approaches, this approach is known as a simple and green method that normally works in various liquids (Zeng et al., 2012), and is capable of producing NPs at a potential rate per minute. It has been shown that liquid medium can play a key role in the size and shape of SnO_2 NPs synthesized by pulsed laser ablation (de Monredon et al., 2002). Also, it has been reported that optical characteristics of SnO_2 NPs fabricated by this method can be influenced by laser ablation time duration and laser power (Desarkar et al., 2012).

Although it has been reported that SnO_2 NPs can show anticancer activities, the signaling pathways involved in the antiproliferative effects of these NPs against breast cancer cells (MCF-7) have not been fully elucidated. Therefore, the main objective and novelty of this work is to explore the anticancer effects of SnO_2 NPs synthesized by pulsed laser ablation method against breast cancer cells (MCF-7) through downregulation of PI3K/AKT/mTOR signaling pathway.

2. Materials and methods

2.1. Materials

3-(4,5-dimethylthiazol-2-yl)-2,5-diphenyl-2H-tetrazolium bromide (MTT), Roswell Park Memorial Institute (RPMI-1640), and fetal bovine serum (FBS) were obtained from Sigma-Aldrich (USA).

2.2. Synthesis of SnO_2 NPs

The synthesis of SnO_2 NPs by pulsed laser ablation technique was done based on a previous report by Tian et al. study (Tian et al., 2011) with some minor modifications. A tin plate was fixed, the vessel filled by 15 ml double distilled water (DDW), ablated for 50 min by 1064 nm Nd:YAG laser with a 8 Hz pulse repetition rate, 5 ns pulse duration, and 100 mJ pulse energy density (Tian et al., 2011). The other remaining set up was similar to the Tian et al. study (Tian et al., 2011).

2.3. SnO_2 NPs characterization

Transmission electron microscopy (TEM, Zeiss, EM10C, 80 KV, Germany) was used to determine the diameter and morphology of SnO_2 NPs. The synthesized NPs were diluted with deionized water, sonicated for 30 min, dropped on carbon coated copper grids, air-dried for 30 min, and the image was taken. The size and charge distribution of synthesized SnO_2 NPs were explored by dynamic light scattering (DLS, Brookhaven, Holtsville, USA). The Fourier transform infrared (FTIR) spectroscopy (SHIMADZU, INDIA) was also done to analyze the vibration modes of Sn-O bonds.

2.4. Cell culture

The MCF-7 and MCF-10A cells were cultured in RPMI-1640 medium containing 10% FBS, and 1% streptomycin and penicillin (100 U/ml) at 37 °C in a 5% CO_2 humidified incubator.

2.5. MTT assay

To explore the SnO_2 NPs-induced cytotoxicity on MCF-7 and MCF-10A, the cells were incubated with varying concentrations of SnO_2 NPs (0.01–100 μg/mL) for 24 hrs. Afterwards, MTT assay was done to measure the viability of cells at 570 employing an ELISA reader (Expert 96, Asys Hitch, Ec Austria).

2.6. ROS assay

The SnO_2 NPs-induced generation of intracellular ROS was investigated based on DCFDA/ H_2DCFDA - Cellular ROS Assay Kit (ab113851). Briefly, after treatments of MCF-7 cells with IC_{50} concentration of SnO_2 NPs, the cells were collected, added by 20 µl of DCFH-DA (30 µM), and incubated for 60 min. The fluorescence intensity of the samples was then assessed using flow cytometry (FACSCalibur; BD Biosciences, San Jose, CA, USA).

2.7. Apoptosis assay

After treatment of cells with IC_{50} concentration of SnO_2 NPs for 24 hrs, cells were collected, re-suspended in 400 µl of Annexin V binding buffer, and added by 10 µl of Annexin V-FITC and. The percentage of apoptotic cells was then determined through flow cytometry (FACSCalibur; BD Biosciences, San Jose, CA, USA).

2.8. Mitochondrial membrane potential assay

The cells were washed in PBS, added by tetraethyl benzimidazolyl carbocyanine iodide (JC-1) solution (10 µM), incubated for 20 min at 37 °C, washed with PBS, treated with IC_{50} concentration of SnO_2 NPs for 24 hrs, and analyzed on a flow cytometry (FACSCalibur; BD Biosciences, San Jose, CA, USA).

2.9. Superoxide dismutase (SOD) and catalase (CAT) activity assays

SOD and CAT assay kits (Abcam, UK) were utilized to assess enzyme activities. Briefly, after treatment of the cells, homogenization, centrifugation, the protein concentration in the supernatant was determined by BCA kit (Sigma, USA). Afterwards, 50 µl of kit reagent was added to 30 µg protein and mixed for 30–60 s at 500 rpm. The absorbance was then read using an ELISA reader (Expert 96, Asys Hitch, Ec Austria).

2.10. Quantitative real time PCR (qRT-PCR) analysis

After treatment of cells, total RNA was extracted using TRIzol reagent (Thermo Fisher Scientific, USA) followed by synthesis of cDNA (RevertAid first-strand cDNA synthesis kit, Takara). The primer sequences are tabulated in Table 1.

qRT-PCR was carried out using an ABI Detection System (Thermo Fisher Scientific) with SYBR® Premix Taq™ II (Takara). The relative expression levels of studied mRNA were normalized relative to GAPDH as a housekeeping gene. The $2^{-\Delta\Delta CT}$ method was used to report the data.

2.11. Western blot analysis

After treatment of the cells, homogenization, and centrifugation at 12,000 rpm for 15 min, protein concentration was calculated by BCA protein assay kit (Thermo, USA). Afterwards, proteins were isolated with SDS-PAGE followed by transferring to polyvinylidene fluoride (PVDF) membrane, soaking in skim milk (5%) for 3 hrs, dipping in primary antibodies (β-actin, Bax, Bcl-2, p-PI3K, p-AKT, p-mTOR, 1:1000, Abcam, UK) diluted with 5% serum protein, shaking for 12 h, and finally incubating for 2 hrs with the secondary antibodies (1:2000, Abcam, USA). After washing, the membrane was used to express the level of proteins using a chemiluminescent imaging analysis system (Thermo Fisher Scientific, USA).

Table 1 Primers used for qRT-PCR.

Gene	Gene Primers used
PI3K	F:5′-GGAAGCCCTCCAGAAAGGTC-3′
	R:5′-GCACTCGGAAGTTGAATGGC-3′
AKT	F:5′-CAGTGGACCACCTTCGTTGA-3′
	R:5′-ACAGAGTCGGCCACTGATTG-3′
mTOR	F:5′-TTCCTGAACAGCGAGCACAA-3′
	R:5′-GTAGCGGATATCAGGGTCAGG-3′
Bax	F:5′-AGCAAACTGGTGCTCAAGGC-3′
	R:5′-CAGGGACATCAGTCGCTTCAG-3′
Bcl-2	F:5′-F-CTTTGAGTTCGGTGGGGTCA-3′
	R:5′-GGGCCGTACAGTTCCACAAA-3′
β-actin	F:5′-TGGAACGGTGAAGGTGACAG-3′
	R:5′-AACAACGCATCTCATATTTGGAA-3′

2.12. Statistical analyses

One-way analysis of variance (ANOVA) was performed by using SPSS and the data were displayed as mean ± SDs. All data were reported as mean ± SD, $n = 5$.

3. Results

3.1. Characterization of synthesized SnO_2 NPs

The diameter and morphology of SnO_2 NPs synthesized by pulsed laser ablation technique in DDW were determined by TEM technique as shown in Fig. 1a. It was shown that synthesized SnO_2 NPs have a size of around 30 nm (based on average diameter of around 200 NPs) with a uniform distribution and spherical morphology. DLS study showed that the size of fabricated SnO_2 NPs in the aqueous solution was around 119 ± 19.37 nm (Fig. 1b) with a zeta potential of around −28.03 ± 7.93 mV (Fig. 1c), revealing the moderate colloidal stability of fabricated NPs. Fig. 1d also displayed the FTIR spectrum of synthesized SnO_2 NPs. It was determined that the bands at 790 and 588 cm^{-1} are associated with the Sn—O and O—Sn—O stretching and bending modes of SnO_2 NPs, respectively (Chand, 2019).

3.2. MTT assay

Fig. 2 displays a concentration-dependent growth inhibition of MCF-7 and MCF-10A cells, whereas this inhibitory effect was more pronounced against MCF-7 cells. The IC_{50} values were determined as 10.03 ± 1.96 µg/mL for SnO_2 NPs -treated MCF-7 cells and > 50 µg/mL for SnO_2 NPs -treated MCF-10A cells. Therefore, for further experiments, the MCF-7 cells were treated with 10 µg/mL of SnO_2 NPs.

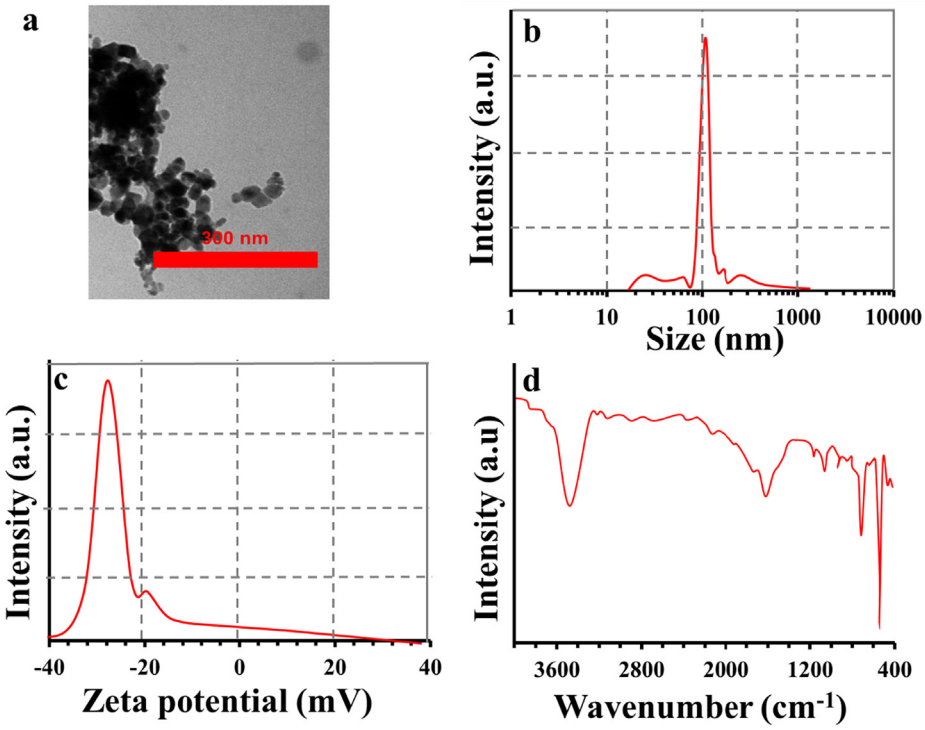

Fig. 1 (a) TEM image, (b) hydrodynamic radius, (c) zeta potential, (d) FTIR spectrum of SnO_2 NPs synthesized by pulsed laser ablation technique.

3.3. ROS and apoptosis assay

The ROS assay demonstrated that the DCF intensity in MCF-7 cells exposed to IC_{50} concentration of SnO_2 NPs (10 μg/mL) for 24 hrs increases, whereas this increase in DCF intensity was inhibited in the presence of NAC (20 μ*M*) (Fig. 3*a*). Statistical analyses indicated there was a significant increase (***P < 0.001) in the generation of ROS upon incubation of cells with SnO_2 NPs, which was remarkably (##P < 0.01) reversed upon co-incubation of SnO_2 NPs-treated cells with NAC (Fig. 3d). Apoptosis induction in MCF-7 cells by SnO_2 NPs was further assessed by flow cytometry assay. Fig. 3C displays that control cells did not show any significant increase in Annexin V fluorescence intensity, whereas SnO_2 NPs -treated cells become apoptotic after 24 hrs as evidenced by a significant increase in the percentage of Annexin$^+$ cells (Fig. 3d). Similarly, co-incubation of SnO_2 NPs-treated cells with NAC resulted in a significant (##P < 0.01) inhibition of apoptosis through reduction of percentage of Annexin$^+$ cells (Fig. 3 c,d).

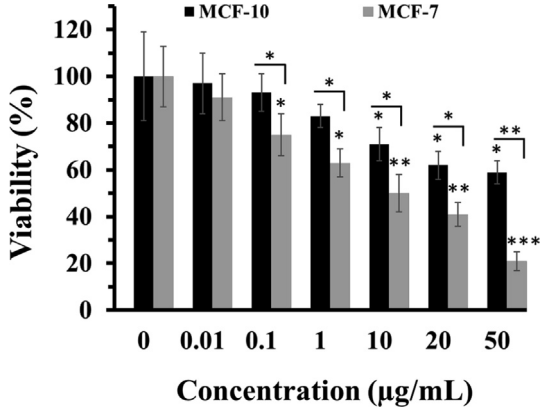

Fig. 2 Effect of SnO_2 NPs on cell viability of MCF-7 and MCF-10A cells. After treatment with different concentrations of SnO_2 NPs ranging from 0.01 μg/ml to 50 μg/ml for 24 hrs, the cell viability was assessed by MTT assay. All data were reported as mean ± SD from five independent experiments. *P < 0.05, **P < 0.01, ***P < 0.001 relative to the control group.

3.4. Enzyme activity and mitochondrial membrane potential assays

The SOD (Fig. 4a) and CAT (Fig. 4b) activities were significantly decreased (**P < 0.01 or ***P < 0.001) in cells exposed to SnO_2 NPs for 24 hrs compared to control cells. Also, the membrane potential was greatly decreased after incubation of MCF-7 with SnO_2 NPs for 24 hrs (Fig. 4c). However, it was seen that the reduction in antioxidant enzyme activity and membrane potential was reversed in the presence of NAC. These results are consistent with ROS and apoptosis assays, suggesting the possible role of ROS in inducing mitochondrial-mediated apoptosis in MCF-7 cancer cells.

3.5. Molecular mechanism

3.5.1. Targeting PI3K/AKT/mTOR signaling pathway

The inhibition of the PI3K/AKT/mTOR pathway could be a potential strategy for cancer treatment (Antonsson, 2001;

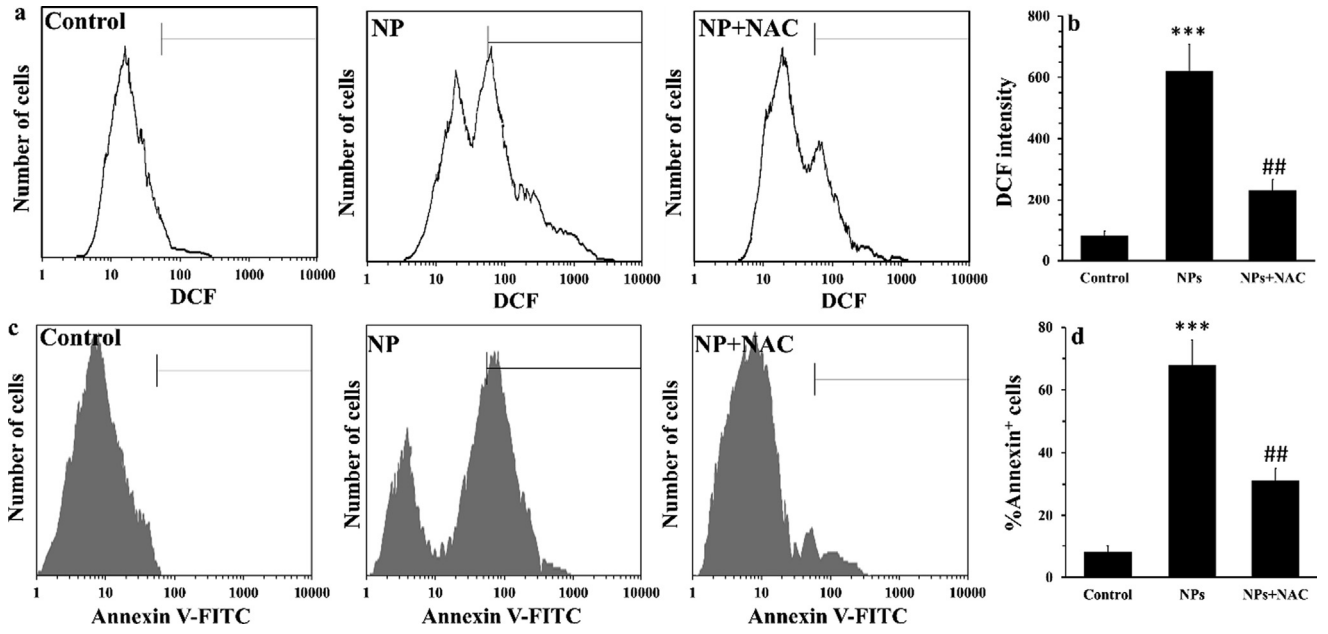

Fig. 3 Effect of the SnO_2 NPs (10 μg/ml) for 24 hrs on ROS production and apoptosis in MCF-7 cells as quantified by flow cytometry. (a) DCF plot, (b) statistical analysis of DCF intensity, (c) Annexin intensity, (d) statistical analysis of Annexin$^+$ cells. ***P < 0.001 relative to the control group; $^{\#\#}$P < 0.01 relative to SnO_2 NP-treated group.

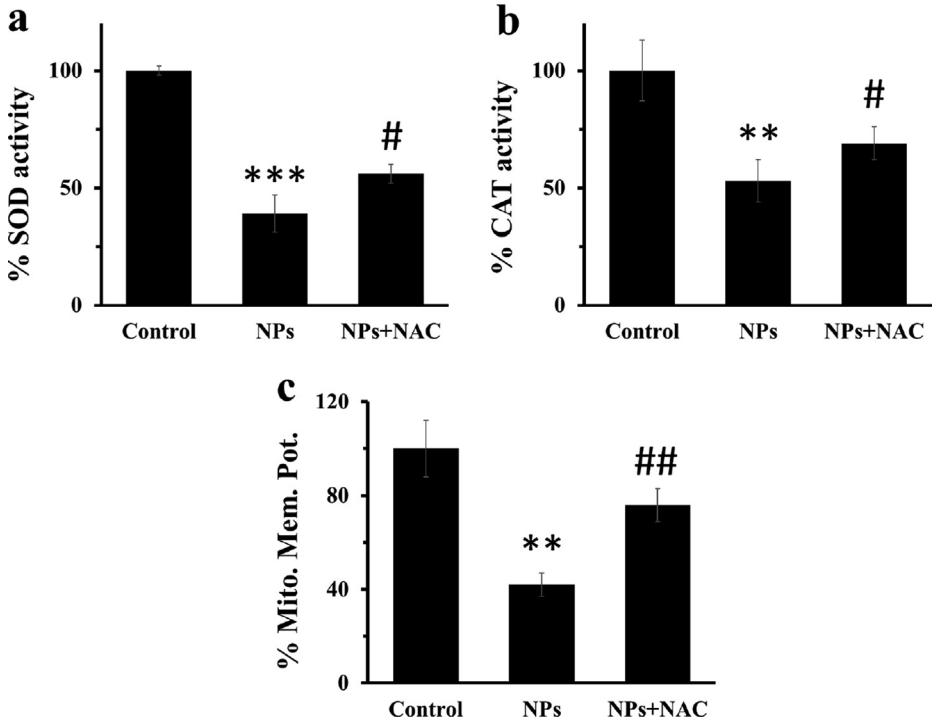

Fig. 4 Effect of the SnO_2 NPs (10 μg/ml) for 24 hrs on SOD and CAT activity as well as mitochondrial membrane potential in MCF-7 cells. (a) SOD activity, (b) CAT activity, (c) mitochondrial membrane potential. **P < 0.01, ***P < 0.001 relative to the control group; $^{\#}$P < 0.5, $^{\#\#}$P < 0.01 relative to SnO_2 NP-treated group.

Sharifi et al., 2020; Porta et al., 2014). We have explored the expression of PI3K, AKT, and mTOR mRNA in the MCF-7 upon incubation with SnO_2 NPs for 24 hrs (Fig. 5a). Our data showed that the MCF-7 cells treated with SnO_2 NPs showed enhanced level mRNA expression for PI3K, AKT, and mTOR (Fig. 5a). Conversely, the expression pattern of protein

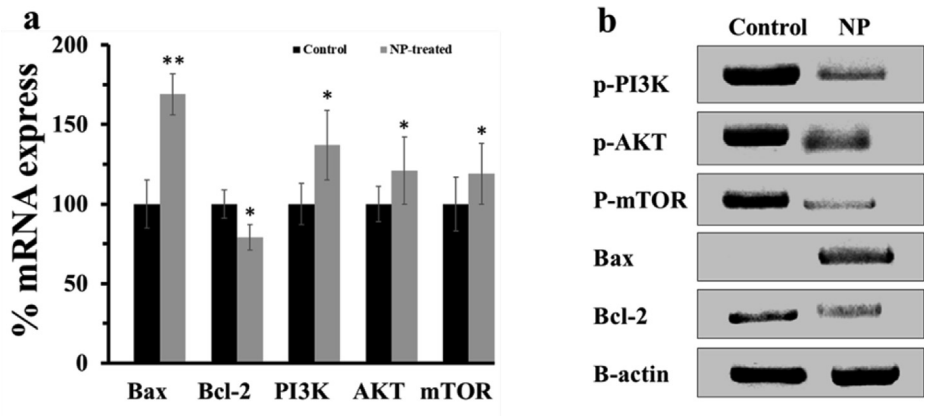

Fig. 5 Effect of the SnO_2 NPs (10 μg/ml) for 24 hrs on mRNA and protein expression in MCF-7 cells. (a) qRT-PCR, (b) western blot. *P < 0.05, **P < 0.01, relative to the control group.

p-PI3K, p-AKT, p-mTOR is downregulated in MCF-7 cells (Fig. 5b).

3.5.2. Targeting mitochondrial dysfunction and apoptosis

Targeting mitochondria can be employed as a promising therapeutic approach for development of anticancer platforms (Costa et al., 2018; Tewari et al., 2019; Mkandawire et al., 2015). In our study, we have examined the probate changes involved in the mRNA and protein expression of Bcl-2 and Bax for MCF-7 upon incubation with SnO_2 NPs for 24 hrs (Fig. 5 a, b). These proteins play a key role in regulating the apoptosis via the mitochondria (Mallick et al., 2018). In our study, the mRNA and protein expression levels of the Bcl-2 was significantly downregulated, whereas, the expression levels of Bax were found to be upregulated upon addition of SnO_2 NPs (Fig. 5 a, b), indicating the probable mitochondrial-mediated apoptosis.

4. Discussion

SnO_2 NPs synthesized by different routes have shown potential anticancer effects (Ahmadabad et al., 2021; Rivas-García et al., 2021; Azimian et al., 2018), but the potential mechanism underlying the cytotoxicity of SnO_2 NPs on breast cancer cells is not well-explored. In our study, a MCF-7 cell was applied to examine cytotoxicity and mechanism of SnO_2 NPs. The outcomes showed that exposure to SnO_2 NPs could lead to cytotoxicity, generate high level of ROS, and cell apoptosis, which was evidenced by flow cytometry assay and changes in mRNA and protein expressions of Bax, Bcl-2, PI3K, AKT, mTOR, p-PI3K, p-AKT and p-mTOR.

The MTT results showed that SnO_2 NPs significantly mitigated cell proliferation in a dose-dependent fashion. Nevertheless, the effects of 0.01 μg/ml and 0.1–10 μg/ml SnO_2 NPs on MCF-7 and MCF-10A cell viability were not statistically significant relative to untreated cells. This data suggests that breast cancer cells may be more sensitive than normal cells in terms of the action of SnO_2 NPs. This selective anticancer effect of SnO_2 NPs can be associated with the mildly acidic microenvironment of cancer cells which result in peroxidase/nanozyme-like activity of NPs (Tammina et al., 2017; Khan et al., 2018; An et al., 2013; Yim et al., 2020).

In order to study whether the increase of cell mortality was linked with the apoptosis induced by Ni NPs through generation of ROS, quantification of ROS, mitochondrial membrane potential, SOD and CAT activity, and detection of apoptosis of MCF-7 cells stained with Annexin-V-FITC were done. Experimental outcomes demonstrated that SnO_2 NPs could induce ROS generation, mitigation of mitochondrial membrane potential, inactivation of SOD and CAT and cell apoptosis, which were reversed in the presence of NAC as a potential antioxidant which was similar to Ahmadabad, Akhtar, Wason and Ahamed' research findings (Ahmadabad et al., 2021; Sharifi et al., 2020; Khan et al., 2020; Akhtar et al., 2012), that was, the apoptosis of cancer cells was induced by different inorganic NPs in such a similar way.

Apoptosis is regulated by exogenous and endogenous pathways, among which mitochondrial-mediated endogenous pathway is known as one of the pivotal pathways of apoptosis (Singh et al., 2019). Bcl-2 protein family can regulate the permeability of the mitochondrial inner membrane (Singh et al., 2019). Bcl-2 protein can mitigate the induction of apoptosis, whereas Bax proteins can elevate apoptosis (Singh et al., 2019). Thus, the ratio of Bax/Bcl-2 can regulate the apoptosis in different cells upon incubation with external stimuli (Singh et al., 2019; Antonsson, 2001). In this study, in comparison to negative untreated cells, the expression of Bax increased, while that of Bcl-2 decreased after exposure to SnO_2 NPs. Meanwhile, cell apoptosis was triggered via mitochondrial -mediated pathway. This data is consistent with the outcomes of other researchers (Liao et al., 2015; Harini et al., 2019).

Numerous studies show that the cytotoxic effects of NPs are induced by regulating the PI3K /AKT/mTOR signaling pathway (Balakrishnan et al., 2017; Duan et al., 2014). Lack of regulation of this pathway leads to the onset of several responses such as growth, proliferation, survival and cell motility, and eventually tumor progression (Porta et al., 2014; Morgensztern and McLeod, 2005; Lee et al., 2015; Zhou et al., 2018). In this study, the anticancer effects of SnO_2 NPs based on the PI3K/AKT/mTOR signaling pathway were investigated. A review of various studies confirms the anticancer effects of NPs by suppressing PI3K activity and then inhibiting AKT activity. Inactivation of this pathway leads to inhibition of other signaling pathways, including mTOR and NF-κB pathways (Morgensztern and McLeod,

2005; Lee et al., 2015; Chan et al., 2019). Inhibition of mTOR and NF-κB activities reduces growth, proliferation, cell invasion, and metastasis (Morgensztern and McLeod, 2005; Lee et al., 2015). Also, downregulation of PI3K/AKT/mTOR signaling pathway in cancer cells inhibits angiogenesis (Tan et al., 2018; Zhu et al., 2020). In the present study, we found that SnO_2 NPs, as active anticancer compounds, can be effective in the prevention and treatment of cancer by downregulation of the PI3K/AKT/mTOR signaling pathway.

Therefore, we speculate that SnO_2 NPs may inhibit the expression of cytokines or signaling transduction pathways based on activating PI3K, which may mitigate the downstream AKT kinase function, and relevant reactions stimulated by AKT. As a result, the limited activation of PI3K/AKT/mTOR pathway leads to over-expressions of proteins including Bax, but down-expression of Bcl-2, eventually leading to apoptosis. Therefore, the use of SnO_2 NPs can be suggested as a treatment with other pharmacological agents.

5. Conclusion

In conclusion, we synthesized SnO_2 NPs as an efficient and potential nanoplatform for inhibition of the PI3K/AKT/mTOR signaling pathway in MCF-7 cells. The most important outcomes of this study are as follows: (i) Synthesized SnO_2 NPs exhibited a selective anticancer effect against MCF-7 cells. (ii) Synthesized SnO_2 NPs have stimulated a mitochondrial-dependent pathway triggering apoptosis. (iii) Synthesized SnO_2 NPs induced their potency in MCF-7 apoptosis through enhanced levels of intracellular ROS generation, deactivation of antioxidant enzymes and decreased mitochondrial potential. (iv) Synthesized SnO_2 NPs inhibited the PI3K/AKT/mTOR signaling pathway in MCF-7 cells. Taken together with these data, we believe that SnO_2 NPs can be used as a potential NP in the development of anticancer systems.

Funding

None.

Declaration of Competing Interest

The authors declare that they have no known competing financial interests or personal relationships that could have appeared to influence the work reported in this paper.

Acknowledgement

The authors acknowledge the Henan Middle-aged Youth Health Technology Innovation Talent Project, No: YXKC2020059 and Top Talent Fund of the Second Affiliated Hospital of Zhengzhou University, No: 2020BJRCA03.

References

Abdel-Rahman, O., 2018. Impact of timeliness of adjuvant chemotherapy and radiotherapy on the outcomes of breast cancer; a pooled analysis of three clinical trials. The Breast. 38, 175–180.

Ahmadabad, L.E., Kalantari, F.S., Liu, H., Hasan, A., Gamasaee, N. A., Edis, Z., Attar, F., Ale-Ebrahim, M., Rouhollah, F., Babadaei, M.M., Sharifi, M., 2021. Hydrothermal method-based synthesized tin oxide nanoparticles: Albumin binding and antiproliferative activity against MCF-7 cells. Mater. Sci. Eng., C 119, 111649.

Akhtar, M.J., Ahamed, M., Kumar, S., Khan, M.M., Ahmad, J., Alrokayan, S.A., 2012. Zinc oxide nanoparticles selectively induce apoptosis in human cancer cells through reactive oxygen species. Int. J. Nanomed. 7, 845.

An, Q., Sun, C., Li, D., Xu, K., Guo, J., Wang, C., 2013. Peroxidase-like activity of Fe3O4@ carbon nanoparticles enhances ascorbic acid-induced oxidative stress and selective damage to PC-3 prostate cancer cells. ACS Appl. Mater. Interfaces 5 (24), 13248–13257.

Ansari, M.A., Badrealam, K.F., Alam, A., Tufail, S., Khalique, G., Equbal, M.J., Alzohairy, M.A., Almatroudi, A., Alomary, M.N., Pottoo, F.H., 2020. Recent nano-based therapeutic intervention of bioactive sesquiterpenes: prospects in cancer therapeutics. Curr. Pharm. Des. 26 (11), 1138–1144.

Antonsson, B., 2001. Bax and other pro-apoptotic Bcl-2 family‘‘ killer-proteins” and their victim the mitochondrion. Cell Tissue Res. 306 (3), 347–361.

Azimian, H., Dayyani, M., Toossi, M.T., Mahmoudi, M., 2018. Bax/Bcl-2 expression ratio in prediction of response to breast cancer radiotherapy. Iranian J. Basic Med. Sci. 21 (3), 325.

Balakrishnan, S., Mukherjee, S., Das, S., Bhat, F.A., Raja Singh, P., Patra, C.R., Arunakaran, J., 2017. Gold nanoparticles–conjugated quercetin induces apoptosis via inhibition of EGFR/PI3K/Akt–mediated pathway in breast cancer cell lines (MCF-7 and MDA-MB-231). Cell Biochem. Funct. 35 (4), 217–231.

Brundha, M.P., Pathmashri, V.P., Sundari, S., 2019. Quantitative changes of red blood cells in cancer patients under palliative radiotherapy-a retrospective study. Res. J. Pharm. Technol. 12 (2), 687–692.

Chan, C.K., Tang, L.Y., Goh, B.H., Kadir, H.A., 2019. Targeting apoptosis via inactivation of PI3K/Akt/mTOR signaling pathway involving NF-κB by geraniin in HT-29 human colorectal adenocarcinoma cells. Progr. Drug Discovery Biomed. Sci. 2(1).

Chand, P., 2019. Effect of pH values on the structural, optical and electrical properties of SnO2 nanostructures. Optik. 181, 768–778.

Costa, R.L., Han, H.S., Gradishar, W.J., 2018. Targeting the PI3K/AKT/mTOR pathway in triple-negative breast cancer: a review. Breast Cancer Res. Treat. 169 (3), 397–406.

de Monredon, S., Cellot, A., Ribot, F., Sanchez, C., Armelao, L., Gueneau, L., Delattre, L., 2002. Synthesis and characterization of crystalline tin oxide nanoparticles. J. Mater. Chem. 12 (8), 2396–2400.

Desarkar, H.S., Kumbhakar, P., Mitra, A.K., 2012. Optical properties of tin oxide nanoparticles prepared by laser ablation in water: Influence of laser ablation time duration and laser fluence. Mater. Charact. 73, 158–165.

Duan, J., Yu, Y., Yu, Y., Li, Y., Wang, J., Geng, W., Jiang, L., Li, Q., Zhou, X., Sun, Z., 2014. Silica nanoparticles induce autophagy and endothelial dysfunction via the PI3K/Akt/mTOR signaling pathway. Int. J. Nanomed. 9, 5131.

Harini, L., Srivastava, S., Gnanakumar, G.P., Karthikeyan, B., Ross, C., Krishnakumar, V., Kannan, V.R., Sundar, K., Kathiresan, T., 2019. An ingenious non-spherical mesoporous silica nanoparticle cargo with curcumin induces mitochondria-mediated apoptosis in breast cancer (MCF-7) cells. Oncotarget. 10 (11), 1193.

Honda, M., Kondo, T., Owashi, T., Shankar, P., Iwamori, S., Ichikawa, Y., Kulinich, S.A., 2017. Nanostructures prepared via laser ablation of tin in water. New J. Chem. 41 (19), 11308–11316.

Khan, S.A., Kanwal, S., Rizwan, K., Shahid, S., 2018. Enhanced antimicrobial, antioxidant, in vivo antitumor and in vitro anticancer effects against breast cancer cell line by green synthesized un-doped SnO2 and Co-doped SnO2 nanoparticles from Clerodendrum inerme. Microb. Pathog. 125, 366–384.

Khan, S., Sharifi, M., Hasan, A., Attar, F., Edis, Z., Bai, Q., Derakhshankhah, H., Falahati, M., 2020. Magnetic nanocatalysts as multifunctional platforms in cancer therapy through the

synthesis of anticancer drugs and facilitated Fenton reaction. J. Adv. Res.
Khan, S., Sharifi, M., Bloukh, S.H., Edis, Z., Siddique, R., Falahati, M., 2020. In vivo guiding inorganic nanozymes for biosensing and therapeutic potential in cancer, inflammation and microbial infections. Talanta 121805.
Kolahalam, L.A., Viswanath, I.K., Diwakar, B.S., Govindh, B., Reddy, V., Murthy, Y.L., 2019. Review on nanomaterials: Synthesis and applications. Mater. Today:. Proc. 18, 2182–2190.
Lee, J.J., Loh, K., Yap, Y.S., 2015. PI3K/Akt/mTOR inhibitors in breast cancer. Cancer Biol. Med. 12 (4), 342.
Liao, W., Yu, Z., Lin, Z., Lei, Z., Ning, Z., Regenstein, J.M., Yang, J., Ren, J., 2015. Biofunctionalization of selenium nanoparticle with dictyophora indusiata polysaccharide and its antiproliferative activity through death-receptor and mitochondria-mediated apoptotic pathways. Sci. Rep. 5 (1), 1–3.
Ma, J., Zhao, M., Zhang, C., Wu, X., Yang, G., 2020. Synthesis of L. Acidissima mediated tin oxide nanoparticles for cervical carcinoma treatment in nursing care. J. Drug Delivery Sci. Technol. 57, 101745.
Mallick, A., Nandi, A., Basu, S., 2018. Polyethylenimine coated graphene oxide nanoparticles for targeting mitochondria in cancer cells. ACS Applied Bio Materials. 2 (1), 14–19.
Mkandawire, M.M., Lakatos, M., Springer, A., Clemens, A., Appelhans, D., Krause-Buchholz, U., Pompe, W., Rödel, G., Mkandawire, M., 2015. Induction of apoptosis in human cancer cells by targeting mitochondria with gold nanoparticles. Nanoscale. 7 (24), 10634–10640.
Morgensztern, D., McLeod, H.L., 2005. PI3K/Akt/mTOR pathway as a target for cancer therapy. Anticancer Drugs 16 (8), 797–803.
Musaev, O.R., Driver, M.S., Sutter, E.A., Caruso, A.N., Wrobel, J. M., Kruger, M.B., 2013. Influence of the liquid environment on the products formed from the laser ablation of tin. Appl. Phys. A 113 (2), 355–359.
Porta, C., Paglino, C., Mosca, A., 2014. Targeting PI3K/Akt/mTOR signaling in cancer. Front. Oncol. 4, 64.
Rivas-García, L., Quiles, J.L., Varela-López, A., Giampieri, F., Battino, M., Bettmer, J., Montes-Bayón, M., Llopis, J., Sánchez-González, C., 2021. Ultra-small iron nanoparticles target mitochondria inducing autophagy, acting on mitochondrial DNA and reducing respiration. Pharmaceutics 13 (1), 90.
Sharifi, M., Jafari, S., Hasan, A., Paray, B.A., Gong, G., Zheng, Y., Falahati, M., 2020. Antimetastatic activity of lactoferrin-coated mesoporous maghemite nanoparticles in breast cancer enabled by combination therapy. ACS Biomater. Sci. Eng. 6 (6), 3574–3584.
Sharifi, M., Hosseinali, S.H., Yousefvand, P., Salihi, A., Shekha, M.S., Aziz, F.M., JouyaTalaei, A., Hasan, A., Falahati, M., 2020. Gold nanozyme: biosensing and therapeutic activities. Mater. Sci. Eng., C 108, 110422.
Singh, R., Letai, A., Sarosiek, K., 2019. Regulation of apoptosis in health and disease: the balancing act of BCL-2 family proteins. Nat. Rev. Mol. Cell Biol. 20 (3), 175–193.
Tammina, S.K., Mandal, B.K., Ranjan, S., Dasgupta, N., 2017. Cytotoxicity study of Piper nigrum seed mediated synthesized SnO2 nanoparticles towards colorectal (HCT116) and lung cancer (A549) cell lines. J. Photochem. Photobiol., B 166, 158–168.
Tan, X., Zhang, Z., Yao, H., Shen, L., 2018. Tim-4 promotes the growth of colorectal cancer by activating angiogenesis and recruiting tumor-associated macrophages via the PI3K/AKT/mTOR signaling pathway. Cancer Lett. 436, 119–128.
Tewari, D., Patni. P., Bishayee, A., Sah, A.N., Bishayee, A., 2019. Natural products targeting the PI3K-Akt-mTOR signaling pathway in cancer: A novel therapeutic strategy. In: Seminars in Cancer Biology. Academic Press.
Tian, Z., Liang, C., Liu, J., Zhang, H., Zhang, L., 2011. Reactive and photocatalytic degradation of various water contaminants by laser ablation-derived SnO x nanoparticles in liquid. J. Mater. Chem. 21 (45), 18242–18247.
Yim, G., Kim, C.Y., Kang, S., Min, D.H., Kang, K., Jang, H., 2020. Intrinsic Peroxidase-Mimicking Ir Nanoplates for Nanozymatic Anticancer and Antibacterial Treatment. ACS Appl. Mater. Interfaces 12 (37), 41062–41070.
Zeng, H., Du, X.W., Singh, S.C., Kulinich, S.A., Yang, S., He, J., Cai, W., 2012. Nanomaterials via laser ablation/irradiation in liquid: a review. Adv. Funct. Mater. 22 (7), 1333–1353.
Zhou, R., Chen, H., Chen, J., Chen, X., Wen, Y., Xu, L., 2018. Extract from Astragalus membranaceus inhibit breast cancer cells proliferation via PI3K/AKT/mTOR signaling pathway. BMC Complementary Altern. Med. 18 (1), 1–8.
Zhu, Y., Liu, X., Zhao, P., Zhao, H., Gao, W., Wang, L., 2020. Celastrol suppresses glioma vasculogenic mimicry formation and angiogenesis by blocking the PI3K/Akt/mTOR signaling pathway. Front. Pharmacol. 11, 25.